IEEE TRANSACTIONS ON MAGNETICS, VOL. 27, NO. 5, SEPTEMBER 1991

# AN EDDY CURRENT CONSTRAINT FORMULATION FOR 3D ELECTROMAGNETIC FIELD CALCULATIONS

Hong Song and Nathan Ida
Department of Electrical Engineering
The University of Akron
Akron, Ohio 44325 U.S.A.

*Abstract* - The use of Coulomb's gauge is sufficient for a unique solution in 3D magnetostatic field calculations in terms of the magnetic vector potential **A**. For the sinusoidal steady-state eddy current problem Coulomb's gauge is not sufficient. The combination of Coulomb's gauge and an eddy current constraint provides a simple way of guaranteeing uniqueness. A formulation for 3D electromagnetic fields utilizing this constraint is proposed. Results comparing the present formulation with other finite element formulations and with experimental data are given.

## INTRODUCTION

The formulation presented here is suitable for finite element computation of eddy current problems and low frequency electromagnetic fields. The magnetic vector potential and the electric scalar potential are used as variables and the solution is rendered unique by use of the coulomb gauge together with a constraint equation on the eddy currents, based on the continuity equation. The formulation is compared with other commonly used formulations, showing more accurate results. The implementation of the method with 8 node hexahedral, isoparametric finite elements is given here. Results are presented for a heating problem where losses in a conductor are calculated and for an eddy current nondestructive testing problem. In the later, the induced voltage in a sensing coil is calculated. These results show good agreement with experimental data.

## FORMULATION

The problem considered here is that of eddy currents and losses at low frequencies. The displacement currents are neglected and permeability is assumed to be constant. Using the magnetic vector potential **A**, the curl-curl equation is

$$\frac{1}{\mu}\nabla\times\nabla\times\mathbf{A} = \mathbf{J}_s + \mathbf{J}_e \tag{1}$$

where $\mu$ is the permeability, $J_S$ is the source current density and $J_e$ is the induced eddy current density

$$\mathbf{J}_e = -\sigma\left(\frac{\partial \mathbf{A}}{\partial t} + \nabla V\right) \tag{2}$$

$\sigma$ is the electric conductivity, and V is the electric scalar potential. In eddy current problems, because eddy currents are not arbitrary, it is very important to restrict the eddy currents in the solution region. This can be done by introducing a constraint equation. A simple way to constrain the eddy currents is to use the current continuity equation

$$\nabla . J_e = 0 \tag{3}$$

as a constraint. The field equation together with the constraint equation are

$$\frac{1}{\mu}\nabla\times\nabla\times\mathbf{A} = \mathbf{J}_s - \sigma\left(\frac{\partial \mathbf{A}}{\partial t} + \nabla V\right) \tag{4a}$$

$$\nabla .\left(\sigma\frac{\partial \mathbf{A}}{\partial t} + \sigma\nabla V\right) = 0 \tag{4b}$$

The solution to equation (4) is not unique, because it does not define the divergence of **A**. Also, the second equation in (4) is not independent. For the eddy current problem, Coulomb's gauge can also be used to enforce the divergence of **A**. Let $\nabla.\mathbf{A}=0$. Then equation (4) becomes

$$-\frac{1}{\mu}\nabla^2\mathbf{A} = \mathbf{J}_s - \sigma\left(\frac{\partial \mathbf{A}}{\partial t} + \nabla V\right) \tag{5a}$$

$$\nabla .\left(\sigma\frac{\partial \mathbf{A}}{\partial t} + \sigma\nabla V\right) = 0 \tag{5b}$$

Equation (5) is the governing equation for the constrained **A**-V formulation.

With $\sigma$=const., and using the gauge transformation, the scalar potential V can be eliminated from equation (4a) or (5a) by defining a modified vector potential **A***.

$$-\frac{1}{\mu}\nabla^2\mathbf{A}^* = \mathbf{J}_s - \sigma\frac{\partial \mathbf{A}^*}{\partial t} \tag{6}$$

where $\mathbf{A}^*=\mathbf{A}+\int_t \nabla V dt$, and $\nabla.\sigma\mathbf{A}^*=0$

Solution to equation (6) cannot guarantee a unique solution for the eddy currents. Since eddy currents are now defined as $\mathbf{J}_e=-\sigma\partial\mathbf{A}^*/\partial t$ a unique solution for eddy currents is only obtained when the boundary conditions are uniquely specified. If $\mathbf{A}_0^*$ (the boundary value of $\mathbf{A}^*$) includes a scalar value, the solution may also include a scalar value. While $\mathbf{B}=\nabla\times\mathbf{A}$ is unique, the eddy current density $\mathbf{J}_e$ may not be unique.

For sinusoidal steady state applications, $\partial/\partial t=j\omega$. The governing equation can be written as

$$-\frac{1}{\mu}\nabla^2.\tilde{\mathbf{A}} = \tilde{\mathbf{J}}_s - j\omega\sigma\tilde{\mathbf{A}} - \sigma\nabla V \tag{7a}$$

$$\nabla.(j\omega\sigma\tilde{\mathbf{A}} + \sigma\nabla V) = 0 \tag{7b}$$

The finite element implementation starts by discretization of the solution domain. The finite elements used here are 8 node, isoparametric hexahedral elements. Using the standard shape functions N for the elements, a weighted residual integral over the element is written as:

$$-\int_v W.\frac{1}{\mu}\nabla^2\widetilde{A}dv = \int_v\left(\frac{1}{\mu}(\nabla\times W).(\nabla\times\widetilde{A}) + \frac{1}{\mu}(\nabla.W)(\nabla.\widetilde{A})\right)dv + \int_s\left(W.\frac{1}{\mu}\nabla\times\widetilde{A}\times\hat{n} + (W.\hat{n})\frac{1}{\mu}(\nabla.\widetilde{A})\right)ds \quad (8)$$

where W is the wighting function.

Applying this to equation (7) gives:

$$\int_v\left(\frac{1}{\mu}(\nabla\times W).(\nabla\times\widetilde{A}) + \frac{1}{\mu}(\nabla.W)(\nabla.\widetilde{A}) + j\omega\sigma W.\widetilde{A} + \sigma W.\nabla V\right)dv - \int_s\left(W.\frac{1}{\mu}\nabla\times\widetilde{A}\times\hat{n} + (W.\hat{n})\frac{1}{\mu}(\nabla.\widetilde{A})\right)ds = \int_v W.J_s dv \quad (9a)$$

$$\int_v\left(j\omega\sigma\nabla W.\widetilde{A}+\sigma\nabla W.\nabla V\right)dv + \int_s W(-j\omega\sigma\widetilde{A}-\sigma\nabla V).\hat{n}ds=0 \quad (9b)$$

The surface integrals in equations (9a) and (9b) imply continuity of the interface conditions $\widetilde{H}\times\hat{n}$, $J_e.\hat{n}$ and $\nabla.\widetilde{A}$ may vanish.

With the weighting functions equal to the shape functions (Galerkin's method), and discretizing equations (9a) and (9b), the following system of equations is obtained:

$$\begin{bmatrix} C + j\omega\sigma D & j\omega\sigma R \\ j\omega\sigma U & j\omega\sigma S \end{bmatrix}\begin{Bmatrix}\widetilde{A} \\ \widetilde{V}\end{Bmatrix} = \begin{Bmatrix}\widetilde{J}_s \\ 0\end{Bmatrix} \quad (10)$$

where the matrices C and D are symmetric matrices and U, R, and S are row vectors.

The formulation above guarantees a unique solution for the magnetic vector potential. This method was applied to a number of problems, for the computation of eddy currents in 3-D geometries. The results for two geometries are given here.

## RESULTS

For comparison purposes, the eddy current losses in an aluminum bar at 60 Hz were calculated and the results compared to three other formulations. The results were also compared to experimental data given in [1].

To compare the results with and without gauge conditions, the following formulations were used:

1. Formulation without gauge condition and without eddy current constraint

$$\frac{1}{\mu}\nabla\times\nabla\times\widetilde{A} = \widetilde{J}_s - j\omega\sigma\widetilde{A} \quad (F1)$$

2. Formulation with Coulomb's gauge included in the equation, no eddy current constraint

$$-\frac{1}{\mu}\nabla^2\widetilde{A} = \widetilde{J}_s - j\omega\sigma\widetilde{A} \quad (F2)$$

3. A-V formulation, no gauge condition, with eddy current constraint

$$\frac{1}{\mu}\nabla\times\nabla\times\widetilde{A} = \widetilde{J}_s - j\omega\sigma\widetilde{A} - \sigma\nabla V \quad (F3a)$$

$$\nabla.(j\omega\sigma\widetilde{A} + \sigma\nabla V) = 0 \quad (F3b)$$

4. A-V formulation with Coulomb's gauge and eddy current constraint

$$-\frac{1}{\mu}\nabla^2\widetilde{A} = \widetilde{J}_s - j\omega\sigma\widetilde{A} - \sigma\nabla V \quad (F4a)$$

$$\nabla.(j\omega\sigma\widetilde{A} + \sigma\nabla V) = 0 \quad (F4b)$$

One octant of the aluminum bar ($\mu_r$=1, $\sigma$=3.54X10$^7$S/m) and excitation coil were modeled. The geometry modeled is shown in Fig. 1. Dimensions are 2.54cm X 2.54cm X 20.32cm for the bar. The coil is 8.128cm long and 0.685cm thick. A complete description of the aluminum bar and the method of measurement of losses are given in [1]. The geometry is divided into 539 first order hexahedral finite elements and 768 nodes. The numerical results for the current formulation (F4), formulations F1-F3 and experimental results are shown in Table 1.

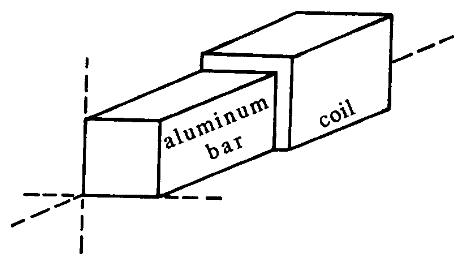


Figure 1. Aluminum bar and coil. One octant of the geometry is shown.

Table 1. Losses in watts in the aluminum bar

| FORMULATION | I = 1Ampere |
|---|---|
| F1 | 0.865 |
| F2 | 0.682 |
| F3 | 1.050 |
| F4 | 0.593 |
| Experimental[1] | 0.580 |

A second problem solved using the formulation presented here is a problem in nondestructive evaluation of materials. The geometry consists of a driving coil with two smaller coils inside the larger, driving coil. The two coils (pickup coils) are connected in opposition to create a differential sensor for the electromagnetic field. This arrangement was used to measure the induced voltage in the differential pair due to defects in conducting materials. The geometry is shown in Fig. 2, together with a test sample. Dimensions for the coils are as follows: driving coil diameter is 44mm, length is 56mm and coil thickness is 4mm. The sensing coils are thin solenoids, 54mm long and 10mm in diameter. A nonconducting frame holds the coils together and provides a separation of 5mm between the coil assembly and the test sample. The test sample is made of stainless steel ($\mu_r$=1, $\sigma$=0.14X10$^7$S/m), 330mm long, 285mm wide and 30mm thick. A flaw is simulated at the center of the sample (i.e. an EDM notch), 40mm long, 0.5mm wide and 10mm deep. The general geometry of the sample is shown in Fig. 2b. Experimental results for this problem have been published[2,6] and other numerical solutions were obtained and compared as part of the TEAM workshop [6].

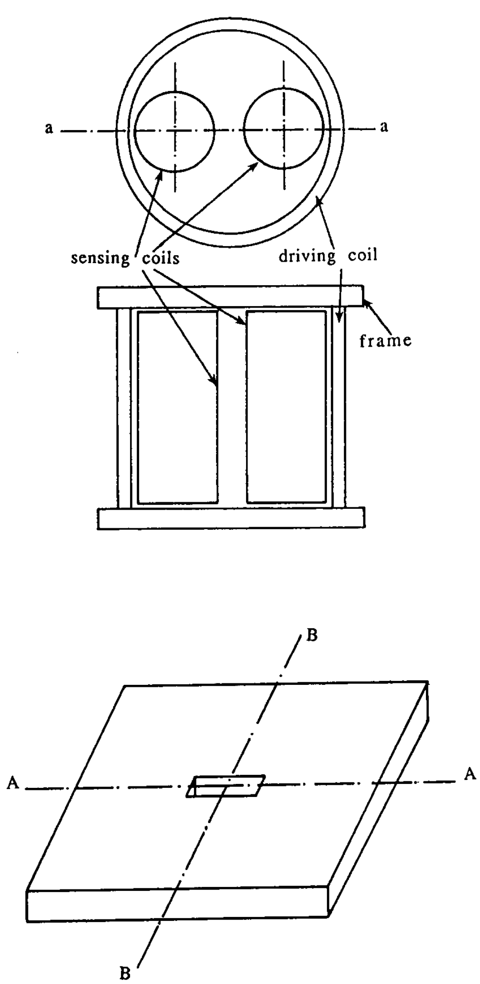


a.

b.

Figure 2. Differential eddy current coil assembly (a) and test sample (b).

Finite Element solutions were obtained for the probe moving parallel and perpendicular to the flaw at 500 Hz. The coils are moved slowly so that the velocity of the coils do not affect the results (experimentally) and there is no need to model the velocity effects numerically. The results for the coil moving parallel to the defect are shown in Fig. 3. In this case, the coil axis a-a moves over the sample axis A-A. The plot represents the imaginary part of the voltage, plotted against the real part. The plot also shows the number of elements and nodes used for the finite element computation. The results for the movement perpendicular to the defect are shown in Fig. 4. In this case, the coil assembly moves such that the coil axis a-a moves over sample axis B-B These results compare very well to both the experimental and other numerical results. A direct comparison of the results presented here and others is available in [6].

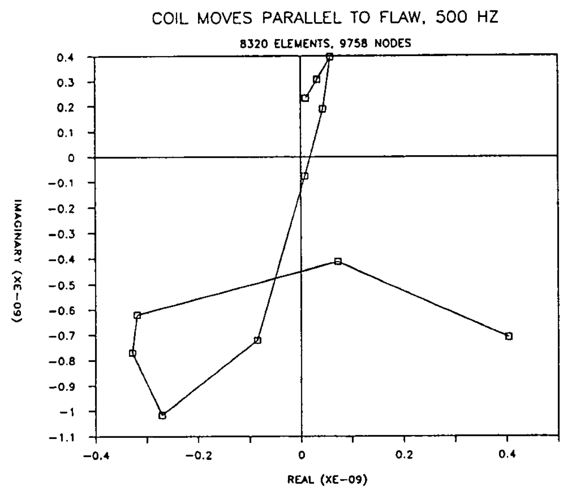


Figure 3. Differential induced voltage in pickup coils for motion parallel to the flaw (A-A axis).

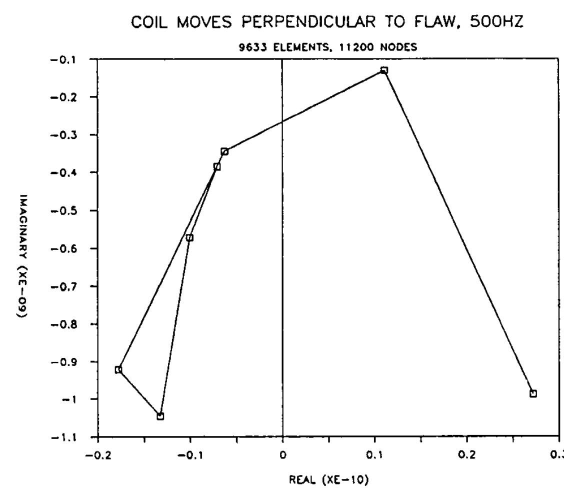


Figure 4. Differential induced voltage in pickup coils for motion perpendicular to the flaw (B-B axis).

## CONCLUSIONS

A simple formulation for eddy current problems based on constrained eddy currents was presented. This formulation provides a unique solution and is applicable to all low frequency eddy current problems. The extension of this formulation to high frequencies is also possible. The results presented show good agreement with experimental data.

REFERENCES

[1] N. A. Demerdash, O. A. Mohammed, T. W. Nehl, F. A. Fouad, R. H. Miller, "Solution of Eddy Current Problems Using Three Dimensional Finite Element Complex Magnetic Vector Potential", IEEE Trans. on Power App. and Syst., Vol. PAS-101, No. 11, pp. 4222-4229, 1982.

[2] J.C. Verite, "Application of a 3-D Eddy Current Code (TRIFOU) to Nondestructive Testing," COMPEL, Vol. 3, pp. 167-178, 1984.

[3] M.V.K. Chari, P. Silvester, A. Konrad, Z. J. Cendes and M. A. Palmo, "Three Dimensional Magnetostatic Field Analysis of Electrical Machinery by the Finite Element Method", IEEE Transactions on Power Apparatus and Systems, Vol. PAS-100, No. 8, pp.4007-4019, 1981.

[4] C. W. Trowbridge, "Status of 3-D Electromagnetic Field Computation", Beijing International Symposium on Electromagnetic Field Computation in Electrical Engineering, pp.3-8, 1988.

[5] O. Biro and K. Preis, "On the Use of the Magnetic Vector Potential in the Finite Element Analysis of Three-Dimensional Eddy Currents", IEEE Transactions on Magnetics, Vol. MAG-25, No. 4, pp.3145-3159, 1989.

[6] Y. Crutzen, N. J. Diserens, C.R.I. Emson and D. Rodger, eds., "Results for TEAM test problem 8", Proceedings of the European Team Workshop and International Seminar on Electromagnetic Field Analysis, Commission of The European Communities, Luxembourg, pp.13-80, 1990.